# Effective Lagrangians :
# A New Approach to $g - 2$ Evaluations

## M. Benayoun

*LPNHE Des Universités Paris VI/VII, IN2P3/CNRS*
*E-mail:* `benayoun@in2p3.fr`

The uncertainty on the theoretical evaluation of the muon anomalous magnetic moment $a_\mu$ is dominated by the contribution of the region covering the non–perturbative regime of QCD. We advocate the use of Effective Lagrangians to improve the knowledge of $a_\mu$ by using global fit methods for the annihilation data at low energies. We specialize to the Hidden Local Symmetry (HLS) Model which is shown to provide a very good simultaneous description of six annihilation channels $e^+ e^- \to H$, where $H = \pi^+ \pi^-$, $\pi^+ \pi^- \pi^0$, $\pi^0 \gamma$, $\eta \gamma$, $K^0 \overline{K^0}$ and $K^+ K^-$ and of the dipion spectrum in the $\tau$ decay. Such a framework allows to yield a solution to the so–called $e^+ e^-$ vs $\tau$ puzzle and permits to address the consistency issue of the various available data samples covering the same annihilation channel. For the channels covered by HLS, which represent more than 80% of the hadronic vacuum polarization, the global approach leads to lessen the uncertainty by $\approx 40\%$ compared to usual methods. Compared to using only the $\pi^+ \pi^-$ scan data, the KLOE data samples increase the significance for a non zero $\Delta a_\mu = a_\mu^{exp} - a_\mu^{th}$ which becomes $> 4.6\sigma$.

## 1. Introduction

The muon anomalous magnetic moment $a_\mu$ has been measured [1, 2] with 0.54 ppm accuracy. An experiment is under construction at FNAL [3] which aims at lowering this accuracy to 0.14 ppm; another experiment, based on a different conceptual design, is also foreseen at J–PARC [4] with the same challenging goal. This raises the issue of deriving theoretical predictions for $a_\mu$ which could compete with the experimental accuracy expected in the near future and, then, could allow to conclude about possible new phenomena beyond the Standard Model.

The predicted value for $a_\mu$ is the sum of several contributions and the most prominent ones are already derived from the Standard Model with very high accuracies. The QED contribution is thus estimated with an accuracy of a few $10^{-12}$ [5, 6, 7] and the precision of the electroweak contribution is now of order $10^{-11}$ [8]. The light–by–light contribution to $a_\mu$ is currently known with an accepted accuracy of $2.6 \times 10^{-10}$ [9].

The issue arises with the contribution of the so–called Hadronic Vacuum Polarization (HVP), especially at low energies. It is admitted that the pertubative regime of QCD (pQCD) starts at some energy around the $J/\psi$ mass region. Then, above some energy threshold where pQCD is supposed to apply, the contribution to the HVP can be computed with a very good accuracy ($\mathscr{O}(10^{-11})$); this should be complemented by the resonance contributions from the $J/\psi$ and $\Upsilon$ regions. However, the energy region up to $\simeq 3$ GeV covers the non–perturbative region of QCD and, here, precise estimates of the HVP derived from QCD *stricto sensu* are lacking. Therefore, the low energy contribution to the leading order HVP (LO–HVP) is evaluated by other means. If one denotes by $\mathscr{H} = \{H_i, i = 1, \cdots n\}$ the set of hadronic states which can be reached in $e^+ e^-$ annihilations, the contribution of each $H_i$ to $a_\mu$ up to some energy cut can be derived using :

$$a_\mu(H_i) = \frac{1}{4\pi^3} \int_{s_{H_i}}^{s_{cut}} ds\, K(s)\, \sigma_{H_i}(s) \;\;, \quad \left[ a_\mu^{LO-HVP} = \sum_i a_\mu(H_i) \right] \tag{1.1}$$

where $s_{H_i}$ is the threshold energy squared of the $H_i$ state, $s_{cut}$ the energy squared above which the pertubative regime of QCD is supposed to start and $\sigma_{H_i}(s)$ is the annihilation cross section $e^+ e^- \to H_i$. $K(s)$ is a known kernel [8] which enhances the effect of the low energy region.

The lay–out of the present study is following. We remind in the short Section 2 the principles of the method which presently underlies the evaluation of the non–perturbative LO–HVP. Section 3 is devoted to sketching what can be expected from Effective Lagrangian approaches covering the non–perturbative regime of QCD; one specializes on the Hidden Local Symmetry (HLS) Lagrangian in Section 4. Section 5 recalls the vector meson mixing mechanism which plays a crucial role in the Broken HLS (BHLS) Model. Special emphasis is put on showing why breaking schemes actually produce intricated effects in processes *a priori* unrelated; how and why this intricacy should underly the model and its associated fitting code is also emphasized. An important issue, the determination of a "reference set of data samples" ($\{R\}$) covering the largest possible physics realm is examined in Section 6. We argue why this reference set $\{R\}$ allows for a critical analysis of possibly conflicting data samples. In Section 7, we illustrate the issue by analyzing the available data samples on the $e^+ e^- \to \pi^+ \pi^-$ annihilation. Section 8 is devoted to our estimates of the muon anomalous moment $a_\mu$ with special emphasis on some minor systematic effects

which can shift its central value. Section 9 is, finally, devoted to conclusions. Some relevant questions raised at the time of the Conference are answered; we also respond to some unappropriate comments at the suitable places.

## 2. Evaluating The Muon Anomalous Magnetic Moment

Up to very recently, the single method used to get the $a_\mu(H_i)$'s was to plug the measured cross sections provided by the various experiments into Eq.(1.1). Among the most recent studies based on this method, let us quote [10, 11, 12]. When several data sets cover the same annihilation process, Eq. (1.1) is either used with some appropriate weighting of the various spectra or by combining the various spectra into a merged one, taking into account the full information provided by each experiment (*i.e.* the spectrum and its full error covariance matrix).

In order to combine safely the various data sets into a single merged spectrum (by means of their own error covariance matrices), such procedures implicitly assume that the various data sets are statistically consistent with each other[1]; stated otherwise, THE DIFFERENT COMBINED DATA SETS ARE SUPPOSED TO BEHAVE AS VARIOUS SAMPLINGS EXTRACTED FROM THE SAME PARENT DISTRIBUTION. This means that the various spectra are supposed not to carry relative inconsistencies (like – possibly local or $s$–dependent – biases) and that each (full) error covariance matrix reflects a reasonably well understanding of the corresponding spectrum. Taking into account the complexity of each experiment and of the data extraction process, this assumption is actually very strong and tools able to ascertain this assumption are certainly valuable.

## 3. Effective Lagrangian Approaches

In order to cover the low energy regime of QCD, a natural approach relies on using Effective Lagrangians constructed in such a way that the symmetry properties of QCD are preserved. Chiral Perturbation Theory (ChPT) represents such a framework valid at very low energies – not much above the $\eta$ mass. As the Resonance Chiral Perturbation Theory (R$\chi$PT) includes vector mesons, this framework can go deeper inside the resonance region; in this case, some parts of the $e^+e^-$ annihilation spectra become accessible to theoretical understanding. It was soon shown [13] that the coupling constants occuring at order $p^4$ in ChPT are saturated by low lying meson resonances of various kinds (vector, axial, scalar, pseudoscalar) as soon as they can contribute. This crucial piece of information emphasizes the role of the fundamental vector meson nonet (V) and confirms the relevance of the Vector Meson Dominance (VMD) concept in low energy physics. On the other hand, Ref. [14] proved that the Hidden Local Symmetry (HLS) model [15] and the Resonance Chiral Perturbation Theory (R$\chi$PT) are equivalent. Therefore, the HLS model is a motivated and constraining QCD inspired framework.

It should be stressed that the Effective Lagrangians just mentioned (as others) share an important common feature which deserves special attention : ALL EFFECTIVE LAGRANGIANS PREDICT

---

[1]Sometimes the claimed uncertainties of some data samples have to be revisited in order to restore an overall consistency.

PHYSICS CORRELATIONS AMONG THE DIFFERENT PHYSICAL PROCESSES THEY CAN ENCOMPASS. This is true before applying symmetry breaking mechanisms and this remains true after.

Therefore, it is natural to analyze experimental data with this perspective in mind. To be clearer, if the same parameters are expected to enter different processes (like $e^+e^- \to \pi^+\pi^-$ and $e^+e^- \to \pi^+\pi^-\pi^0$ and $e^+e^- \to K\overline{K}$ and $\pi^0/\eta/\eta' \to \gamma\gamma$ and $\eta/\eta' \to \pi^+\pi^-\gamma \dots$), it looks appropriate to analyze the experimental data using models which implement *as such* the common parameters in the various possible physics channels where they should occur. This motivates the use of simultaneous analyses/fits of the largest possible set of annihilation data covering the largest possible number of different processes. Proceeding this way, one can indeed check whether each given parameter accepts to carry the same value in all processes where it is supposed to play some role as can be inferred from the Effective Lagrangian framework used.

Because of the global character generated by the physics correlations among various channels, (global) Effective Lagrangian approaches allow, in principle, for several improvements while analyzing data, because :

- (**1**) As the model parameters are common to several processes, all processes (and the associated data) contribute to determine their central values, their uncertainties and their error covariance matrix. Therefore, the model parameters become certainly (much) better defined than when using each process separately.

- (**2**) Provided that some set of data samples yields an acceptable global solution using fitting methods, it can serve to examine additional data sets and check their consistency with the rest of the physics involved (in the same channel as well as in all the other channels correlated by the same model).

- (**3**) If one is using several tens of different data sets, collected with different detectors, by different groups using different data extraction methods and tools, one may think that the effects of unidentified experimental systematics will be either detected or, when marginal, averaged appropriately; it looks, indeed, unlikely that systematics associated with a large number of independent data samples will not be distributed and could simply pile up.

As for the evaluation of $g-2$, which is our primary concern, item # **1** above has potentially important consequences : If a given model leads to a perfect description of the data, it becomes motivated to replace in Eq.(1.1) above the experimental cross sections by their model partners and, using the fit parameter values and error covariance matrix, one should obtain improved estimates for the various $a_\mu(H_i)$. The credibility of the numerical results derived from the fit parameters and their error covariance matrix should be reflected by the quality of global fit tags like the fit probability.

## 4. The HLS Framework And Its Breaking

Even if in its original form [15] the HLS Lagrangian is clearly motivated, the level of accuracy reached by the data supposes to supply it with symmetry breaking schemes which may allow for refined descriptions. For instance, the non–anomalous sector of the original HLS Lagrangian depends on only two parameters (*a* and *g*) which is clearly insufficient for physics studies beyond

formal properties; as a trivial example, without some symmetry breaking, the decay constant ratio $f_K/f_\pi$ has no way to depart from 1.

On the other hand, the HLS model has a validity range which cannot go much beyond the $\phi$ mass. It is thus of concern to check that possible low energy effects of higher mass vector mesons do not prevent HLS to reach a good account of all data up to the $\phi$ mass region. Analyzing their $e^+e^- \to \pi^+\pi^-$ data, the CMD–2 Collaboration compared the HLS pion form factor [16] and the more traditional Gounaris–Sakurai (GS) [17] expression supplemented with some higher mass $\rho$ contribution. Their fit results [18] illustrates that both descriptions are statistically good and strikingly equivalent; this means either that higher mass $\rho$ contributions below the GeV are negligible or that they are effectively absorbed by the constant term of the HLS pion form factor. Similarly, our own study [19] relying on all data then available, confirmed that the HLS framework was indeed performing well[2].

Later on, Refs. [20, 21, 22, 23] have proved that the global HLS model was, indeed, able to account simultaneously for 6 annihilation channels ($e^+e^- \to \pi^+\pi^-$, $e^+e^- \to (\pi^0/\eta)\gamma$, $e^+e^- \to \pi^+\pi^-\pi^0$, $e^+e^- \to K^+K^-$ and $e^+e^- \to K^0\overline{K}^0$) and the dipion spectrum in the $\tau$ decay. This proved that the breaking mechanisms applied to the various pieces of the HLS Lagrangian are consistent and well accepted by $\approx 40 \div 50$ different data sets covering seven physics spectra up to $\simeq 1.05$ GeV – and some more vector or pseudoscalar meson decay properties (see [23] and previous references herein).

As complementary topics, the HLS model has provided [21, 24] valuable predictions for the dipion spectra in the $\eta/\eta' \to \pi^+\pi^-\gamma$ decays, while mixing fit results from the pion form factor and information from the Wess-Zumino-Witten Lagrangians. On the other hand, several results derived using the HLS model [19, 25, 26] are found in good agreement with the corresponding pieces of information derived by ChPT or Extended ChPT (EChPT) [27, 28] from quite different input data.

Stated otherwise, the broken HLS model (BHLS) has successfully passed a large number of tests and has always been found in good correspondence with independent expectations.

## 5. Some Features Of The Broken HLS Model

As stated above, in order to become operative, the HLS model must be supplied with breaking schemes. Some are generalizations of the so–called BKY mechanism [29, 30, 31] which have been discussed in detail elsewhere[3]. We rather put here some emphasis on the breaking mechanism more specific to vector mesons, the vector meson mixing (VMM) [20, 23] within the HLS framework. This should apply *mutatis mutandis* to any Effective Lagrangian framework implementing vector mesons as explicit degrees of freedom.

### 5.1 The Vector Meson Mixing (VMM) Mechanism

The VMM mechanism is motivated by two issues. The former is the presence of the $\omega$ and $\phi$ signals in the $e^+e^- \to \pi^+\pi^-$ annihilation, admittedly attributed to an isospin 1 component inside the $\omega$ and $\phi$ mesons. Similarly, the $\rho^0 \to \pi^+\pi^-\pi^0$ decay is interpreted as a small isospin 0

---

[2]Loop corrections, later identified as $\gamma - \rho$ mixing [10], were accounted for and shown to significantly improve the fit quality.

[3]See [30, 25, 20, 21, 22, 23, 26] for the various aspects.

component inside the $\rho^0$. The latter issue is the long reported discrepancy between the pion form factor in the $e^+e^-$ annihilation and in the $\tau$ lepton decay.

Within the HLS model, VMM is generated mostly (but not only) by kaon loop effects which, beside self–mass effects, generate non–diagonal entries in the vector meson (squared) mass matrix. As all vector mesons inside the original HLS Lagrangian couple to kaon pairs, they undergo transitions from one to each other and then, the original vector meson fields are no longer mass eigenstates[4] at one–loop order. The relation between both kinds of fields can be written :

$$
\begin{pmatrix} \rho_I \\ \omega_I \\ \phi_I \end{pmatrix} = \begin{pmatrix} 1 & -\alpha(s) & \beta(s) \\ \alpha(s) & 1 & \gamma(s) \\ -\beta(s) & -\gamma(s) & 1 \end{pmatrix} \begin{pmatrix} \rho_R \\ \omega_R \\ \phi_R \end{pmatrix} \tag{5.1}
$$

where the mixing "angles" depend on the invariant mass flowing through the vector meson line and fulfill the real analyticity condition $f^*(s^*) = f(s)$. Within HLS, the mixing angles depend on the charged ($L^\pm$) and neutral ($L^0$) kaon loops. The $\rho_I - \omega_I$ and $\rho_I - \phi_I$ mixing angles, resp. $\alpha(s)$ and $\beta(s)$, depend on $L^\pm - L^0$, while the $\omega_I - \phi_I$ mixing angle $\gamma(s)$ depends on $L^\pm + L^0$.

It deserves to note that isospin breaking (IB) in the pseudoscalar sector generates a non–vanishing difference $L^\pm - L^0$. Therefore, the mechanism which generates isospin 1 components inside the $\omega$ and $\phi$ mesons and an isospin 0 component inside the $\rho^0$ is IB *in the pseudoscalar sector*. In contrast, the usual $\omega - \phi$ mixing is generated by loop effects independently of any kind of IB. As a general statement, VMM is always *s*–dependent.

### 5.2 Intricacy Of Symmetry Breaking Effects

As just illustrated with kaon loops, symmetry breaking effects in some sector may generate effects in *a priori* unrelated sectors. This seems to be a general feature which is worth further examplifying. For this purpose, let us display some BHLS Lagrangian pieces given in [23]. The interaction between the *physical* neutral vector fields and a pion pair is governed by :

$$
\mathscr{L}_1 = \frac{iag}{2}(1 + \Sigma_V) \left[ \{\rho^0 + [\varepsilon_\pi - \alpha(s)] \ \omega + \beta(s) \ \phi\} \cdot \pi^- \overset{\leftrightarrow}{\partial} \pi^+ \right], \tag{5.2}
$$

and the transitions from *physical* neutral vector mesons to photons are derived from :

$$
\mathscr{L}_2 = -e \left[ f_{\rho\gamma}(s)\rho^0 + f_{\omega\gamma}(s)\omega - f_{\phi\gamma}(s)\phi \right] \cdot A \tag{5.3}
$$

where :

$$
\begin{cases} f_{\rho\gamma}(s) = agf_\pi^2 \left[ 1 + \varepsilon_\rho + \dfrac{\alpha(s)}{3} + \dfrac{\sqrt{2}z_V}{3}\beta(s) \right] , \\[2ex] f_{\omega\gamma}(s) = \dfrac{agf_\pi^2}{3} \left[ 1 + \varepsilon_\omega - 3\alpha(s) + \sqrt{2}z_V \ \gamma(s) \right] , \\[2ex] f_{\phi\gamma}(s) = \dfrac{agf_\pi^2}{3} \left[ -\sqrt{2}z_V + 3\beta(s) + \gamma(s) \right] , \end{cases} \tag{5.4}
$$

---

[4]For convenience, the original vector fields will carry a subscript *I* and the physical vector fields – *i.e.* eigenstates of the (squared) mass matrix at one loop order – a subscript *R* or no subscript.

$\Sigma_V$, $\varepsilon_\pi$, $\varepsilon_\rho$ and $\varepsilon_\omega$ are isospin breaking *constants* of little concern for the present purpose; they can be fixed to zero, as they were in the early version of BHLS [20, 21, 22]. Likewise, the SU(3) breaking constant $z_V$ generated by the BKY mechanism can be replaced by 1.

Finally, the $\rho^\pm$ interaction with a pion pair looks *mutatis mutandis* like for the $\rho^0$, and the $\rho^\pm − W^\pm$ transition amplitude – which mediates the $\tau$ decay – is given by $f_{\rho W} = ag f_\pi^2 [1 + \Sigma_V]$, identical to $f_{\rho\gamma}(s)$ when there is no vector mixing[5].

Eqs. (5.2–5.4) exhibit how the mixing "angles" $\alpha(s)$, $\beta(s)$ and $\gamma(s)$ come in. One thus observes a tight connection between the $\omega/\phi \to \pi^+\pi^-$ and $\omega/\phi \to e^+e^-$ couplings. Indeed the vector meson couplings to a lepton pair are given by $F_{V\gamma}^e(m_V^2)/m_V^2$ where :

$$F_{V\gamma}^e = f_{V\gamma}(s) - \Pi_{V\gamma}(s) \quad , \quad (V = \rho^0, \, \omega, \, \phi) \qquad (5.5)$$

The second term, which is a usual important piece of the HLS amplitudes [19, 20, 21], is what has been identified as $\gamma − V$ mixing and studied specifically in [10]. In addition to the connexion between the dipion and $e^+e^-$ couplings of the $\omega$ and $\phi$ mesons, one should note that the mixing "angles" play a crucial role in the $\rho^0 \to e^+e^-$ coupling and, thus, at all energies in $e^+e^- \to H_i$ transitions. Stated otherwise, IB effects generating the $\omega/\phi \to \pi^+\pi^-$ decays strongly influence the whole description of the $e^+e^-$ annihilation data. Thus, a global unified framework allows to ascertain that the description of all relevant data remains self–consistent.

## 6. The Reference Set Of Data Samples ({$R$})

In order to work, the BHLS model needs to have fixed (explicit) breaking parameters and coefficients of several subtraction polynomials of pseudoscalar loops, presently a total[6] of 24 quantities. As there is generally no deep theoretical motivation to fix them precisely, almost all parameter values should be 100 % data driven[7].

This poses the problem of having a reliable reference set of data samples ({$R$}) which allows to derive credible parameter values. Because of the intricacy pattern illustrated above, the only way is to perform a *global* fit of the corresponding set of data samples, fully using the whole information provided with each data sample (in particular, its full error covariance matrix). In this case, as one can minimize a global $\chi^2$ function reflecting at best the whole experimental knowledge, the probability returned by the minimization procedure is already a first (legitimate) tag. However, because of a possibly weak statistical weight of some (group of) data samples $A$, a good global fit probability might hide a poor description of $A$ and, therefore, one is also led to privilege an

---

[5]The IB effects affecting specifically the $\tau$ spectra, the so–called short–range and long–range effects or the pion mass difference are treated as usual in the literature; the other effects (essentially the $\rho$ mass and width differences) are accounted for as explained in [23, 26]. IB effects affecting the $\tau$ physics play no role in the breaking schemes specifically implemented in BHLS as clear from [21] – which simply ignores $\tau$ physics – and from [22, 23, 26] where estimates of the same physics quantities derived using or discarding the $\tau$ data are provided.

[6]For comparison, the Extended Gounaris–Sakurai parametrization used by Belle [32] to account for their spectrum involves 10 parameters for 62 data points. It is, therefore, clear that 24 parameters to account for seven different spectra and a few more meson partial widths – $\simeq 800$ data points in total – does not reflect an inflating freedom.

[7]Practically, the only parameters carrying definite values within BHLS are $\alpha_{em}$, $G_F$ and the pseudoscalar meson masses.

auxiliary tag specific of $A$. We have chosen $\chi_A^2/N_A$, the average $\chi^2$ at minimum for the data subset A; this is requested not to depart "too much" from 1.

Table 3 in [23] proves that all existing data[8] covering the 5 annihilation channels $e^+e^- \to \pi^0/\gamma$, $e^+e^- \to \eta\gamma$, $e^+e^- \to \pi^+\pi^-\pi^0$, $e^+e^- \to K^+K^-$ and $e^+e^- \to K^0\overline{K}^0$ together with all existing *scan* data for $e^+e^- \to \pi^+\pi^-$ (referred to as NSK in the following) provide a quite satisfactory "Reference Set of Data Samples" $\{R\}$ for BHLS. Indeed, submitting $\{R\}$ to the global fit procedure constructed from BHLS, all parameters of the model yield satisfactory values and the parameter error covariance matrix allows a motivated estimate of the uncertainties of derived quantities.

As for the role of the available $\tau$ spectra collected[8] by ALEPH, CLEO and Belle, it deserves to remind that they have not mandatorily to be included in $\{R\}$ in order for HLS to provide fair evaluations of physics parameters like $g-2$. Indeed, as reported in Table 3 of [22], these $\tau$ spectra are precisely predicted by the HLS model (already in its earlier form [22]) using only $\{R\}$. This allowed to conclude that there is no visible mismatch between $e^+e^-$ and $\tau$ data within BHLS; this conclusion has been enforced by updating the HLS breaking procedure [23].

As the $\tau$ spectra are clearly well understood within the BHLS framework [23, 26], there is no reason to give up using them to improve physics quantity values; in this case, the reference data set is extended in order to include the quoted $\tau$ spectra and is referred to as $\{R\}_\tau$.

The probabilities reached when fitting $\{R\}/\{R\}_\tau$ within the BHLS framework are above the 90% level due to the highly favorable $\chi^2$ obtained for some group of data sets (in particular, all data for $e^+e^- \to \eta\gamma$ and $e^+e^- \to \pi^0\gamma$). Concerning the scan data from CMD–2 and SND for $e^+e^- \to \pi^+\pi^-$, the global BHLS model returns the average $[\chi^2/N]_{SND+CMD2} = 128.3/127 = 1.01$ and a global fit probability at 96% ($\{R\}_\tau$) and, correspondingly, $[\chi^2/N]_{SND+CMD2} = 123.6/127 = 0.97$ and a global fit probability at 99% ($\{R\}$).

Therefore the "Reference Set of Data Samples" $\{R\}/\{R\}_\tau$ defined just above allows confidently to conclude that the constraints imposed to the data by the BHLS model are quite satisfactorily fulfilled.

As a closing remark, it should be stressed that, even keeping in mind that BHLS is a phenomenological model which should/can be improved, one can hardly consider as purely accidental its remarkable simultaneous account of all the physics channels up to and including the $\phi$ region.

## 7. Differential Behavior Of The Various $e^+e^- \to \pi^+\pi^-$ Data Samples

As stated above, $\{R\}$ contains $40 \div 50$ independent data samples. Most of the corresponding spectra are covered by several independent data samples; the consistency of these data samples among themselves and with the other spectra has been addressed and the conclusions can be found in [21, 23]; similarly, the 3 replicas of the $\tau$ dipion spectrum contained in $\{R\}_\tau$ were examined in [22] and they were found in reasonable accord up to $\simeq 1$ GeV.

Concerning the $e^+e^- \to \pi^+\pi^-$ annihilation channel which is of prime concern because of the overwhelming contribution of $a_\mu(\pi\pi)$ to $g-2$, a huge experimental effort has taken place since almost 20 years and is expected to be carried on at BESIII in Beijing and in Novosibirsk by CMD–

---

[8] See [23] for a detailed list of references.

3 and SND in a near future. As for their accuracy[9], the most important data samples have been collected by CMD–2 [34, 35] and SND [36] on VEPP–2M at Novosibirsk in scan mode; they have been followed by higher statistics data samples collected in the ISR mode by the KLOE/KLOE–2 experiments running on DAΦNE [37, 38, 39] and by the BaBar experiment running on PEP2 [40, 41].

For our concern, the issue is : How each of these spectra (each accompanied by its error covariance matrix as provided by each experiment) behaves when included inside our "Reference Set Of Data Samples" $\{R\}$ and/or $\{R\}_\tau$ ? We already know, as reported in [23] and reminded in the previous Section, that the CMD–2 and SND data samples[10] behave consistently within BHLS with the rest of $\{R\}$ and $\{R\}_\tau$ and lead to quite remarkable fit qualities.

If any, the issue is then the behavior of the various ISR data samples when considered within $\{R\}$ and $\{R\}_\tau$. In the following these are referred to as KLOE08 [37], KLOE10 [38], KLOE12 [39] and BaBar [40, 41].

### 7.1 $\tau$ Based Predictions

Let use name for conciseness $\{R'\}$ and $\{R'\}_\tau$ the "Reference Sets Of Data Samples" amputated from all $e^+e^- \to \pi^+\pi^-$ data samples. An interesting topic is to examine how BHLS fed with $\{R'\}_\tau$ predicts the pion form factor as measured in $e^+e^-$ annihilations. This is nothing but the converse of what has been done in [20, 22] using only the $\pi^+\pi^-$ scan data; it was then shown that annihilation data allow for a fair prediction of the $\tau$ dipion spectra.

The BHLS model contains the breaking effects generated by the BKY mechanism [29, 30, 31], by the determinant terms breaking the nonet symmetry in the pseudoscalar sector [42] and, finally, by VMM (the vector meson mixing) [20, 23]. As already stated, almost all model parameter values are data driven, especially those hidden inside the VMM "angles" $\alpha(s)$, $\beta(s)$ and $\gamma(s)$.

In spite of the intricacy emphasized in Subsection 5.2, the specific IB effects occuring in the $e^+e^- \to \pi^+\pi^-$ annihilation are only marginally constrained by the information carried by $\{R'\}$ or $\{R'\}_\tau$. So specific pieces of information have to be provided to BHLS in order that it can provide a valuable prediction of the $e^+e^- \to \pi^+\pi^-$ annihilation.

It is obvious [26] that data related with the $\omega/\phi \to \pi^+\pi^-$ decays have mandatorily to be fed; these certainly include the corresponding branching ratios and the (Orsay) phases between the $\omega/\phi$ amplitudes and the underlying coherent $\pi^+\pi^-$ background. Less obvious but as mandatory : A piece of information expressing the distortion between the $\rho^\pm$ ($\tau$) spectrum and the $\rho^0$ ($e^+e^-$) spectrum should also be provided; the $\rho^0 \to e^+e^-$ partial width is the obvious candidate. Of course, because of the intricacy phenomenon, this input influences in turn the $\gamma - V$ transitions amplitudes and thus the description of all data contained in $\{R'\}$ or $\{R'\}_\tau$.

Using, mostly[11] the accepted values extracted from the Review of Particle Properties (RPP) [43], BHLS is able to provide an overall satisfactory prediction for the pion form factor $F_\pi^e(s)$ as illustrated by Figure 1. As all data from $\{R'\}_\tau$ submitted to the BHLS fit only cover the energy region from threshold to the $\phi$ mass, the leftmost panel in Figure 1 clearly proves that the so–called

---

[9]The data samples formerly collected with the CMD and OLYA detectors at Novosibirsk and reported in [33] are also considered; they influence the fits only marginally.

[10]As a whole, the CMD–2, SND, CMD and OLYA are referred to as NSK.

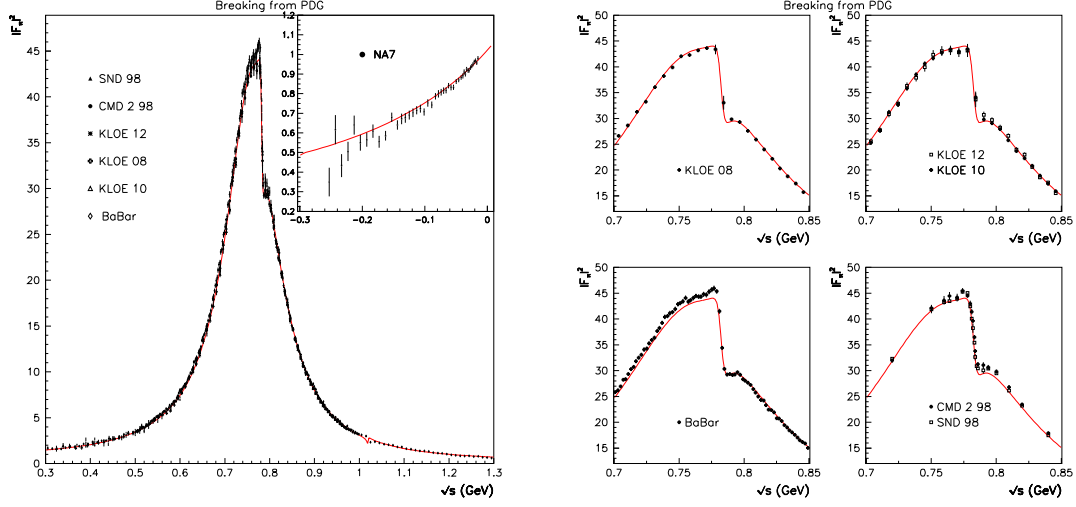[11]There is no entry for Orsay phases in the RPP.

**Figure 1:** The Pion Form Factor *prediction* based on $\tau$ data and PDG information. The most important experimental data are superimposed; they do not influence the predicted curve. The rightmost panel displays, magnified, the pattern in the $\rho - \omega$ interference energy region.

$\tau$ +PDG predictions extend quite satisfactorily to the spacelike region and also somehow above the $\phi$ mass.

The rightmost panel in Figure 1 magnifies the $\tau$ +PDG prediction and the data in the $\rho - \omega$ interference region. It is quite obvious that this panel exhibits sensitive differences in the $\rho$ peak region between the various data samples, the interpretation of which should be dealt with some care.

A first striking feature is that the central values of the KLOE08 data points follow *perfectly* the $\tau$ +PDG prediction and that the data points from KLOE10 and KLOE12 follow *almost* as well the predicted curve. One also observes a clear issue with the BaBar data; indeed while the high mass wing and a large part of the fall–off region is well accounted for by the prediction, the central values of the data points in the $0.74 \div 0.78$ GeV region exhibit a shift. One should also note that the scan data (CMD–2 and SND) look slightly shifted vertically. As we know (see Section 6) that NSK perfectly accomodates BHLS, this gives a hint that one has to go beyond PDG information which may carry some bias relative to specific data. Moreover, the correlations carried by the error covariance matrix are not displayed while they play an important role in the fit procedure.

## 7.2 Global Fits with Isolated and/or Combined $\pi^+ \pi^-$ Data Samples

From the discussion outlined just above, one clearly observes that, overall, the $\tau$+PDG prediction is good; however, nothing more conclusive can be firmly stated, at least because of the bin–to–bin correlations which can hardly be displayed. Ref. [26] reports on BHLS global fits using, together with data samples $\{R'\}_\tau$ or $\{R'\}$, the available $\pi^+ \pi^-$ data samples isolatedly and

combined. This work concluded to inconsistencies between KLOE08 and BaBar (up to 1 GeV), on the one hand, and the rest of the physics involved in the global fit, on the other hand.

However, the newly issued KLOE12 $\pi^+\pi^-$ data sample [39] deserves an update and the present work outlines the first study of its behavior. Table 1 reminds the most relevant properties already known for NSK and KLOE10 [26] together with the corresponding ones derived for KLOE12. The first two data lines in Table 1 display the fit results using $\{R'\}_\tau$ and, respectively, each of the NSK, KLOE10 and KLOE12 data samples in turn. In this case, each of the NSK, KLOE10 and KLOE12 samples yields an average $\chi^2$ per $(\pi^+\pi^-)$ data point of $\approx 1$ and comparable global fit probabilities – of the order 90% or higher.

| Fit Condition | NSK & KLOE10 & KLOE12 | | |
| --- | --- | --- | --- |
| Ref. Channels+ | NSK (127) | KLOE10 (75) | KLOE12 (60) |
| single ($\chi^2/N$) | 1.01 **[0.97]** | 0.98 **[0.92]** | 1.06 **[1.06]** |
| single (fit Prob.) | 96.3 % **[99.4%]** | 87.7 % **[97.8%]** | 92.1% **[95.4%]** |
| combined ($\chi^2/N$) | 1.06 **[1.01]** | 0.95 **[0.98]** | 1.06 **[1.07]** |
| combined (fit Prob.) | 93.1% **[98.2%]** | | |

**Table 1:** Fit results using the set of reference channels $\{R'\}_\tau$ supplemented with the indicated $\pi^+\pi^-$ data samples either alone (first two lines) or combined (last two lines). The number of data points in each data set is given within brackets in the Table subtitles. The boldfaced numbers within square brackets are derived by fitting $\{R'\}$ – *i.e.* excluding the $\tau$ spectra – within BHLS.

The last 2 data lines in Table 1 show the outcome of the BHLS global fits when $\{R'\}_\tau$ is complemented with NSK & KLOE10 & KLOE12. One observes that the average $\chi^2$ per $\pi^+\pi^-$ data point for each of these does not change by more than $\approx 5\%$ compared with their value in fits where they are considered separately; additionally, the global fit probability is also almost unchanged. This is typically what can be expected if these 3 objects were extracted from a same parent distribution. The upmost panels in Figure 2 show the global fit performed by using either of KLOE10 and KLOE12 separately; the downmost panels illustrates the fit quality when using simultaneously NSK & KLOE10 & KLOE12.

### 7.3 The $\pi^+\pi^-$ Data Samples : Closing Remarks

When analyzed within the BHLS global context, the various available $\pi^+\pi^-$ data samples happen to be split up into two groups. The first one gathers CMD–2, SND, KLOE10 and KLOE12 which behave in full compliance with each other and with all data from $\{R'\}$ (or even $\{R'\}_\tau$) and covers 6 different physics spectra fed by more than 40 data samples. The other contains the KLOE08 and BaBar (up to 1 GeV only) samples. As these happen to exhibit some difficulty to accomodate the rest of the physics, we have preferred discarding them.

Therefore, in order to derive reliably physics quantities from BHLS global fits, it is clearly motivated to include within $\{R\}_\tau$ only the CMD–2, SND, KLOE10 and KLOE12 data samples for
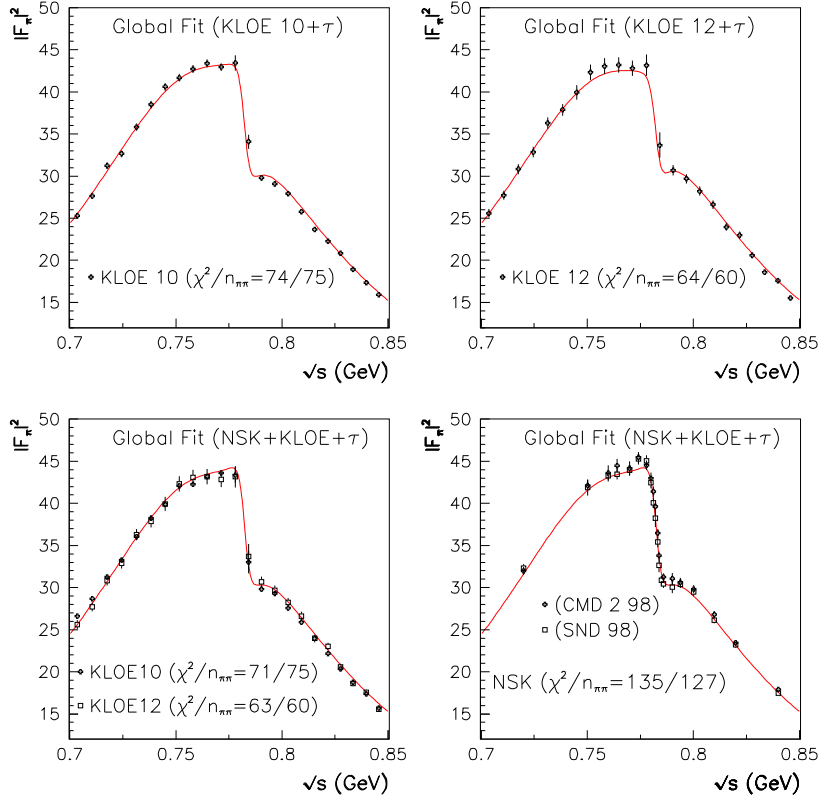
**Figure 2:** Global fit behavior of the KLOE10 & KLOE12 data samples in isolation within the global BHLS context (upper panels); downmost panels show the case when using simultaneously NSK & KLOE10 & KLOE12. One should note how the $\chi^2/N$ varies for KLOE10 & KLOE12 between fits in isolation (upper panels) and when combined with NSK (bottom left panel).

the important and crucial $\pi^+\pi^-$ channel. In this case, as one does not observe any kind of tension between all the data samples treated, one may legitimately expect that the central values for the physics estimates are unbiased and their error estimates reliable. One should indeed stress that the information coded in the minimization procedure is the whole reported experimental information (spectrum & covariance matrix) and nothing else; additionally, as the fit does not detect any kind of tension among the $\approx 50$ data samples contained in $\{R\}_\tau$, one can conclude that the VMD constraints are smoothly satisfied.

## 8. The Muon Anomalous Moment $a_\mu$

The BHLS model encompasses 6 annihilation cross sections (to the $\pi^+\pi^-$, $\pi^0\gamma$, $\eta\gamma$, $\pi^+\pi^-\pi^0$, $K^+K^-$ and $K^0\overline{K}^0$ final states) which can be accurately fitted up to 1.05 GeV. The con-

tribution of the corresponding intermediate states to $a_\mu$ up to this energy are computed using Eq. (1.1) together with the BHLS cross sections. Using the fit output (parameter central values and error covariance matrix), the various $a_\mu(H_i, [s_{H_i}, 1.05 \text{ GeV}])$ are computed by performing $10\,000$ Monte Carlo samplings. Some annihilation channels not accounted for by the present BHLS also contribute to $a_\mu$; the contribution of these missing channels [23, 26] up to 1.05 GeV is small and has been estimated[12] to $1.55 \pm 0.57$, using traditional methods.

Therefore, BHLS is expected to provide an optimal evaluation of the Leading Order HVP (LO–HVP) contribution to the muon $g − 2$ up to 1.05 GeV. As the realm covered by BHLS carries more than 80% of the total HVP, the improvement should be substantial. The total LO–HVP is derived by adding the contribution of the region $[1.05, \infty]$ which amounts to $112.96 \pm 4.13$ [23]. All other contributions to $g − 2$ are listed in Table 7 from [26].

As the BHLS global fit already considers the full experimental error covariance matrices when dealing with data, the uncertainty it provides merges already all *reported* experimental statistical and systematic errors; there is no way to split up the two pieces.
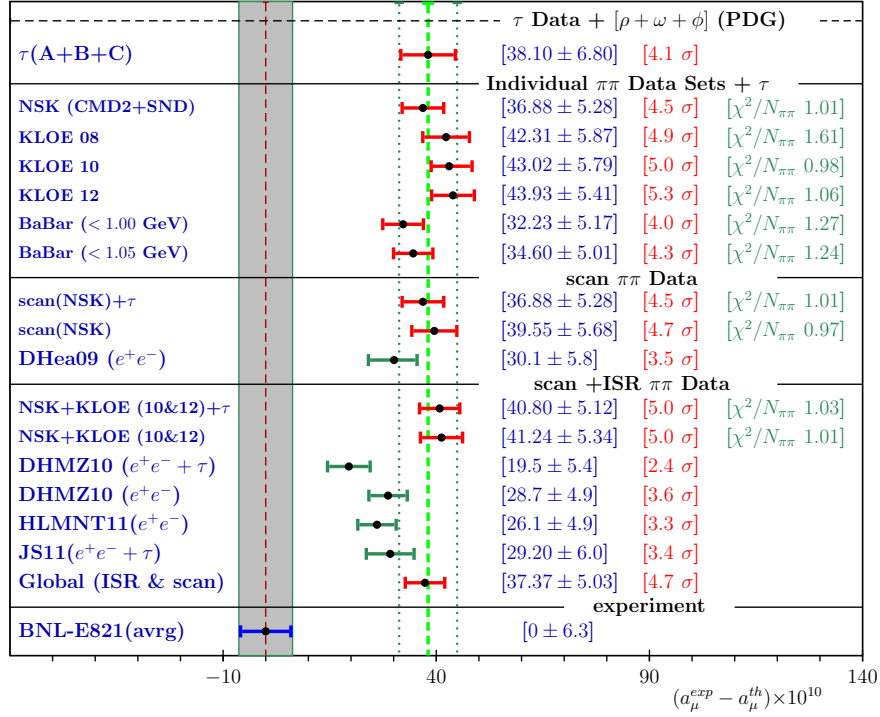


**Figure 3:** Values and significance for $\Delta a_\mu = a_\mu^{exp} - a_\mu^{th}$ derived using as $\pi^+\pi^-$ data the samples those listed in the first column; NSK actually contains also the former data samples from CMD and OLYA. On top, the value for our $\tau$+PDG estimate based on the data from ALEPH (A), CLEO (C) and Belle (B). Evaluations derived by other groups are also shown (see [26] for references).

---

[12]In this Section, all contributions to $a_\mu$ are given in units of $10^{-10}$.

Other sources of systematics exist, some related with the poor experimental knowledge of some spectra (*i.e.* the $\phi$ region of the $\pi^+\pi^-$ spectrum, for instance), some others related with using $\tau$ spectra. These have been already discussed in [26] and will simply be reused. Here, we will rather discuss specific BHLS systematics recently identified.

A common feature of these additional systematics is that they should not be merged with the theoretical error derived from the BHLS fits, as they essentially play as a possible shift of the central value for $a_\mu$.

## 8.1 The Muon $g − 2$ : The Central Value And its Uncertainty

Figure 3 displays the central value, its uncertainty and the significance for $\Delta a_\mu = a_\mu^{exp} - a_\mu^{th}$, where $a_\mu^{th}$ is computed as sketched just above and, for the non–perturbative contributions up to 1.05 GeV, using Eq. (1.1) with the theoretical cross section and the parameters extracted from the global fit. Its uncertainty is derived by means of Monte Carlo methods using 10000 samplings of the parameter error covariance matrix. For completeness, the experimental value is [1, 2] $a_\mu^{exp} = 11\,659\,208.9 \pm 6.3$.

One has found useful to display our final results for NSK and NSK+KLOE10+KLOE12, using *or not* the $\tau$ data. One should note a shift of 2.67 units between the two cases for NSK; this shift, which was still [26] 2.00 when using NSK+KLOE10, reduces to 0.44 when using NSK+KLOE10+KLOE12; this allows to improve the (possible) shift due to using the $\tau$ data from 2 to 0.44 units. The ordering is always $a_\mu^{th}(e^+e^-) > a_\mu^{th}(e^+e^- + \tau)$ as could be expected [26]. Finally, the "$\tau$ + PDG" prediction displayed on top of Figure 3 does not exhibit any significant mismatch with none of our favored configurations (NSK or NSK+KLOE10+KLOE12).

## 8.2 Hunting For (Additional) Systematics On The Muon $g − 2$

Several experimental groups have published their estimate of the contribution to $a_\mu(\pi^+\pi^-)$ from the $0.630 \div 0.958$ GeV region. We do likewise, as it is the best way to look for BHLS specific systematics over the most important energy range. The left–hand panel of Figure 4 displays the experimental evaluations of $a_\mu(\pi^+\pi^-, [0.630, 0.958]$ GeV) and the BHLS estimates derived using $\{R\}_\tau$. Because of some controversy, we have also found worth showing the BHLS estimates derived using only $\{R\}$; this could indicate some issue with the $\tau$ data (if any).

One observes a good matching between data and the $\{R\}_\tau$ BHLS evalutions in all cases (even for Babar if one limits oneself to fitting up to 1. GeV). One should also note that the corresponding ($\{R\}_\tau$–BHLS) and ($\{R\}$–BHLS) evaluations are in good compliance. The difference between them decreases from using solely NSK to using NSK+KLOE10+KLOE12. In this last case, $\{R\}_\tau$ and $\{R\}$ evaluations through BHLS almost coincide.

This may indicate that the difference between fitting $\{R\}_\tau$ or $\{R\}$ with BHLS is of statistical origin. Therefore, one does not see any reason to hesitate using the $\tau$ data, as it corresponds to increasing the statistics without any detectable consistency issue.

As for the interest of using an Effective Lagrangian framework : Comparing the BHLS value for $a_\mu(\pi^+\pi^-, [0.630, 0.958]$ GeV) to its experimental partner (within parentheses) exhibits a quite substantial gain for the uncertainty. The uncertainty returned by BHLS is always 40% smaller than its experimental partner (derived using traditional methods).
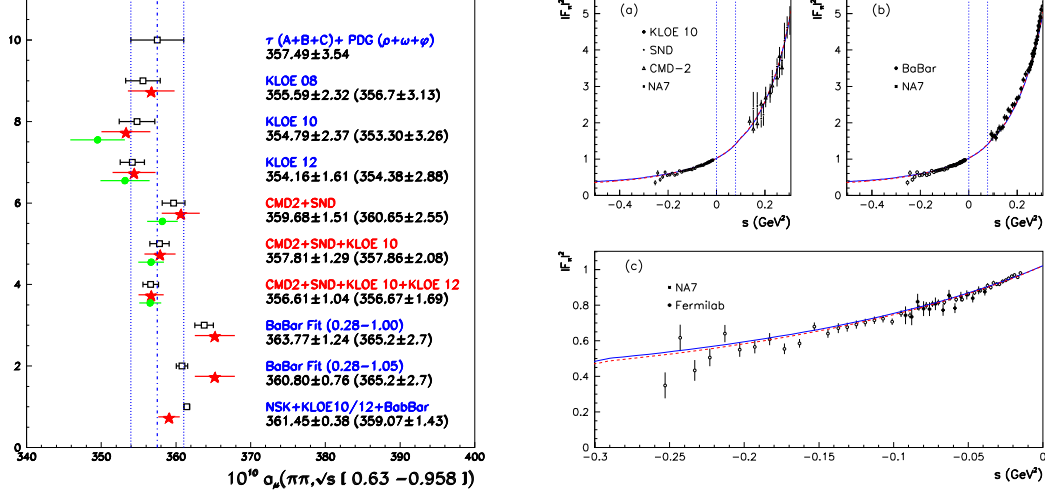
14

**Figure 4:** The left–side panel displays the various evaluations of $a_\mu(\pi^+\pi^-)$ from the $0.630 \div 0.958$ GeV region. Red stars are the experimental estimates, black squares the BHLS evaluations based on $\{R\}_\tau$; full green circles are BHLS evaluations derived excluding $\tau$ ($\{R\}$). The right–side panel shows the continuation of the BHLS best fit based on $\{R\}_\tau$ (with NSK+KLOE10+KLOE12) down to the threshold and its prediction in the spacelike region.

The right–hand panel of Figure 4 shows how our fitting function extends down to the threshold and, even, into the spacelike region where it is a *prediction*. One can hardly detect a disagreement with data or an unexpected behavior.

However, comparing the phase of $F_\pi(s)$ derived from the BHLS fit with data and other reliable predictions, especially the one derived from ChPT predictions, could give a more sensitive test of the very low energy behavior.

The left–hand panel in Figure 5 shows the phase of $F_\pi(s)$ as derived from the BHLS fit together with the available data [44, 45]; also displayed are the phase shift (CGL) derived from ChPT [46], those derived from the Roy equations and from the fit (JS11) performed in [10].

The general behavior of the BHLS prediction is noticeably very good up to 1.2 GeV, much beyond our fitting range and closer to the data than others. The inset, however, indicates some limited issue interestingly related with a peculiarity of the BHLS model in its present form : The strict equality of the Lagrangian (HK) masses for the $\rho^0$ and $\omega$ mesons generates a small bump ($\approx 1°$ amplitude) close to 350 MeV. In this case, the mixing angle $\alpha(s)$ does not vanish at $s = 0$ (in contrast with $\beta(s)$ and $\gamma(s)$) and, moreover, behaves as shown in Figure 6 of [21]. This can be cured by imposing such a mass difference. Indeed, the right–hand panel in Figure 5 shows, for instance, the case when plugging into the fitting code $[m_\omega^{HK}]^2 = (1 + \eta)[m_\rho^{HK}]^2$ with $\eta = 5\%$. On the other hand, the $\varepsilon_\pi$ (see Eq. (5.2)) breaking parameter plays some role at $s = 0$. As these two issues are somewhat correlated, we have performed a few fits varying these. For instance, $\eta = 5\%$
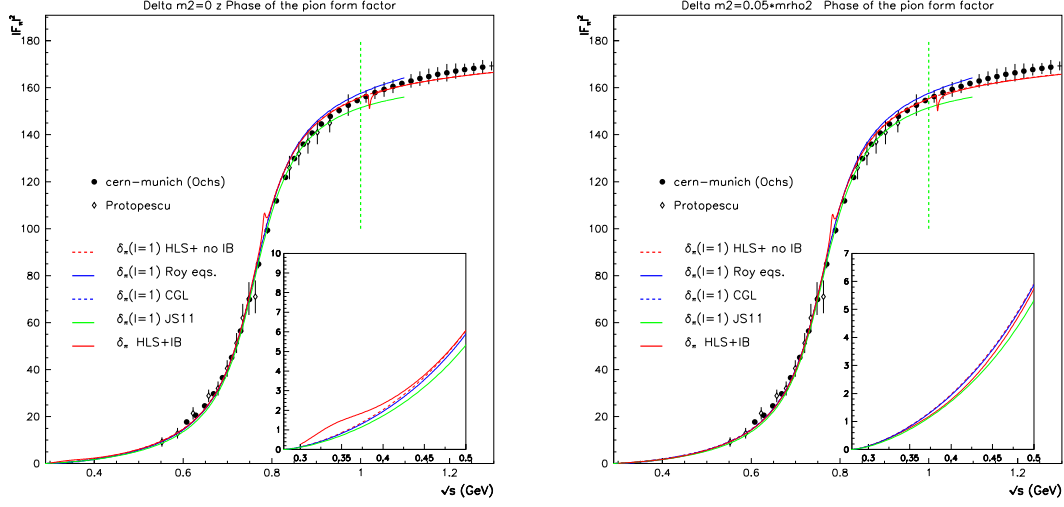
**Figure 5:** Phase–shift data, estimates from [46] and [10] together with our own estimates. The insets magnify the various behaviors close to threshold. See text for more explanations.

and $\varepsilon_\pi = 0$ lead to :

$$F_\pi^e(s) =_{s\to 0} 1 + as + bs^2 \tag{8.1}$$

with $a = 1.77\,\mathrm{GeV}^{-2}$ and $b = 4.07\,\mathrm{GeV}^{-4}$ – both laying in the expected range – and to an improved account of the spacelike data (in terms of $\chi^2$). This specific study leads to estimates of $a_\mu^{th}(\pi^+\pi^-)$ which could undergo an increase by $\delta a_\mu^{th}(\pi^+\pi^-) \simeq 1.4 \div 2.2$.

The issues just reported strongly motivates to slightly extend the BHLS model breaking to include nonet symmetry breaking in the vector sector. In this case, the $\delta a_\mu^{th}(\pi^+\pi^-)$ systematics just referred to will be naturally absorbed into the model; one also may expect an interesting influence on the description of the spacelike data.

### 8.3 Final Results For The Muon $g − 2$

Gathering all the results sketched above, the final results can be expressed as :

$$\Delta a_\mu(NSK + KLOE\,10/12) = 40.80 + \left[^{+0.6}_{-1.3}\right]_\phi + \left[^{+0.4}_{-0.0}\right]_\tau + \left[^{+0.0}_{-2.2}\right]_{ChPT} \pm 5.12_{th} \pm 6.3_{exp}$$

$$\tag{8.2}$$

$$\Delta a_\mu(NSK) = 36.88 + \left[^{+0.6}_{-1.3}\right]_\phi + \left[^{+0.4}_{-0.0}\right]_\tau + \left[^{+0.0}_{-2.2}\right]_{ChPT} \pm 5.28_{th} \pm 6.3_{exp}$$

($\Delta a_\mu = a_\mu^{exp} - a_\mu^{th}$) where $a_\mu^{exp} = 11\,659\,208.9$ and all numbers being written in units of $10^{-10}$. As the systematics just discussed come as a possible shift of the central value, this means that the significance is bounded from below by $\Delta a_\mu > 4.6\sigma$ for NSK+KLOE10+KLOE12, while it is $\Delta a_\mu > 4.2\sigma$ when limiting oneself to the scan data only.

16

## 9. Conclusions

The most important conclusion which can be drawn from our work is that Effective Lagrangians allow for significant improvements in physics studies, especially for important quantities like $g-2$. Even if derived within the BHLS framework, some properties are certainly valid within other global frameworks. For instance, because Effective Lagrangians imply physics correlations among the various cross sections, all spectra contribute to the determination of each of the model parameters. Compared to traditional methods which ignore such correlations, this approach is equivalent to having a much larger statistics; in the case of BHLS, this can be estimated to a $3 \div 4$ times increase, without any increase of systematics, always a delicate matter.

Concerning the results more specifically related with the Broken HLS (BHLS) Model, several conclusions have been reached which can be summarized as follows :

- The annihilations channels entering its realm, namely $e^+e^- \to \pi^+\pi^-$, $e^+e^- \to \pi^+\pi^-\pi^0$, $e^+e^- \to \pi^0\gamma$, $e^+e^- \to \eta\gamma$, $e^+e^- \to K^0\overline{K^0}$ and $e^+e^- \to K^+K^-$ have been successfully and simultaneously accounted for – based on $\approx 50$ independent data samples – and with quite good fit probabilities.

- Within BHLS, one does not find any discrepancy between the $e^+e^-$ annihilation and $\tau$ decay dipion spectra. This proves that this long standing puzzle vanishes if isospin breaking is suitably defined; the role of the vector meson mixing is crucial in order to reach this conclusion.

- In the HLS range of validity, bounded by $\approx 1.05$ GeV, the improvement of the uncertainty on the HVP evaluation is close to a factor of 2 compared to more usual error estimates. One should also note that using the $\tau$ data produces a significant improvement of the uncertainties, as can be seen in Figure 3. Some further improvement can be expected when new data, especially covering the $\phi$ mass region, will become available.

  Nevertheless, it is clear that the theoretical uncertainty on $g-2$ becomes dominated by the HVP uncertainty coming from the energy region above the $\phi$ meson (presently $4.13 \times 10^{-10}$). Compared to this, further improving the accuracy in the region up to the $\phi$ will not produce visible effects. Fortunately, CMD–3, SND and BESSIII may change the picture.

- Our final result concerning the muon anomalous moment is

$$\Delta a_\mu(NSK + KLOE\,10/12) = 40.80 + [^{+0.6}_{-1.3}]_\phi + [^{+0.4}_{-0.0}]_\tau + [^{+0.0}_{-2.2}]_{ChPT} \pm 5.12_{th} \pm 6.3_{exp} \quad (9.1)$$

  ($\Delta a_\mu = a_\mu^{exp} - a_\mu^{th}$ with $a_\mu^{exp} = 11\,659\,208.9$). The theoretical estimated error merges the effects of all reported experimental statistical and systematic errors. The (additional) systematics given here play by possibly shifting the central value. Our evaluation for $a_\mu$ leads to a significance for $\Delta a_\mu \neq 0$ which is larger than $4.6\sigma$; limiting oneself to only the scan data, this bound reduces to $4.2\sigma$, showing the effects of the KLOE data samples.

# References

[1] MUON G-2 collaboration, G. W. Bennett et al., *Final report of the muon E821 anomalous magnetic moment measurement at BNL*, *Phys. Rev.* **D73** (2006) 072003, [hep-ex/0602035].

[2] B. Lee Roberts, *Status of the Fermilab Muon $(g − 2)$ Experiment*, *Chin. Phys.* **C34** (2010) 741–744, [1001.2898].

[3] FERMILAB P989 COLLABORATION collaboration, B. Lee Roberts, *The Fermilab muon (g-2) project*, *Nucl.Phys.Proc.Suppl.* **218** (2011) 237–241.

[4] J-PARC NEW G-2/EDM EXPERIMENT COLLABORATION collaboration, H. Iinuma, *New approach to the muon g-2 and EDM experiment at J-PARC*, *J.Phys.Conf.Ser.* **295** (2011) 012032.

[5] T. Aoyama, M. Hayakawa, T. Kinoshita and M. Nio, *Tenth-Order QED Contribution to the Electron g-2 and an Improved Value of the Fine Structure Constant*, *Phys.Rev. Lett.* **109** (2012) 111807, [1205.5368].

[6] T. Aoyama, M. Hayakawa, T. Kinoshita and M. Nio, *Complete Tenth-Order QED Contribution to the Muon g-2*, *Phys.Rev. Lett.* **109** (2012) 111808, [1205.5370].

[7] M. Passera, *Precise mass-dependent QED contributions to leptonic g-2 at order $\alpha^2$ and $\alpha^3$*, *Phys.Rev.* **D75** (2007) 013002, [hep-ph/0606174].

[8] F. Jegerlehner and A. Nyffeler, *The Muon g-2*, *Phys. Rept.* **477** (2009) 1–110, [0902.3360].

[9] Joaquim Prades, Eduardo de Rafael and Arkady Vainshtein, *Hadronic Light-by-Light Scattering Contribution to the Muon Anomalous Magnetic Moment*, 0901.0306.

[10] F. Jegerlehner and R. Szafron, *$\rho^0 − \gamma$ mixing in the neutral channel pion form factor $|F_\pi|^2$ and its role in comparing $e^+e^−$ with $\tau$ spectral functions*, *Eur. Phys. J.* **C71** (2011) 1632, [1101.2872].

[11] T. Teubner, K. Hagiwara, R. Liao, A. D. Martin and D. Nomura, *Update of g-2 of the muon and Delta alpha*, *Chin. Phys.* **C34** (2010) 728, [1001.5401].

[12] K. Hagiwara, R. Liao, A. Martin, D. Nomura and T. Teubner, *$(g − 2)_\mu$ and $\alpha(M_Z^2)$ re-evaluated using new precise data*, *J.Phys.* **G38** (2011) 085003, [1105.3149].

[13] G. Ecker, J. Gasser, A. Pich and E. de Rafael, *The Role of Resonances in Chiral Perturbation Theory*, *Nucl.Phys.* **B321** (1989) 311.

[14] G. Ecker, J. Gasser, H. Leutwyler, A. Pich and E. de Rafael, *Chiral Lagrangians for Massive Spin 1 Fields*, *Phys.Lett.* **B223** (1989) 425.

[15] M. Harada and K. Yamawaki, *Hidden local symmetry at loop: A new perspective of composite gauge boson and chiral phase transition*, *Phys. Rept.* **381** (2003) 1–233, [hep-ph/0302103].

[16] M. Benayoun et al., *New results in $\rho^0$ meson physics*, *Eur. Phys. J.* **C2** (1998) 269–286, [hep-ph/9707509].

[17] G. J. Gounaris and J. J. Sakurai, *Finite width corrections to the vector meson dominance prediction for $\rho \to e^+e^−$*, *Phys. Rev. Lett.* **21** (1968) 244.

[18] CMD-2 collaboration, Aulchenko V. M.and others, *Measurement of $e^+e^− \to \pi^+\pi^−$ cross section with CMD-2 around rho meson*, *Phys. Lett.* **B527** (2002) 161–172, [hep-ex/0112031].

[19] M. Benayoun, P. David, L. DelBuono, P. Leruste and H. B. O'Connell, *The pion form factor within the Hidden Local Symmetry model*, *Eur. Phys. J.* **C29** (2003) 397–411, [nucl-th/0301037].

[20] M. Benayoun, P. David, L. DelBuono, O. Leitner and H. B. O'Connell, *The Dipion Mass Spectrum In $e^+e^-$ Annihilation and tau Decay: A Dynamical ($\rho^0$, $\omega$, $\phi$) Mixing Approach*, Eur. Phys. J. **C55** (2008) 199–236, [hep-ph/0711.4482].

[21] M. Benayoun, P. David, L. DelBuono and O. Leitner, *A Global Treatment Of VMD Physics Up To The $\phi$: I. $e^+e^-$ Annihilations, Anomalies And Vector Meson Partial Widths*, Eur. Phys. J. **C65** (2010) 211–245, [0907.4047].

[22] M. Benayoun, P. David, L. DelBuono and O. Leitner, *A Global Treatment Of VMD Physics Up To The phi: II. $\tau$ Decay and Hadronic Contributions To g-2*, Eur. Phys. J. **C68** (2010) 355–379, [0907.5603].

[23] M. Benayoun, P. David, L. DelBuono and F. Jegerlehner, *Upgraded Breaking Of The HLS Model: A Full Solution to the $\tau^- - e^+e^-$ and $\phi$ Decay Issues And Its Consequences On g-2 VMD Estimates*, Eur.Phys.J. **C72** (2012) 1848, [1106.1315].

[24] M. Benayoun, P. David, L. DelBuono, P. Leruste and H. B. O'Connell, *Anomalous $\eta/\eta'$ decays: The triangle and box anomalies*, Eur. Phys. J. **C31** (2003) 525–547, [nucl-th/0306078].

[25] M. Benayoun, L. DelBuono and H. B. O'Connell, *VMD, the WZW Lagrangian and ChPT: The third mixing angle*, Eur. Phys. J. **C17** (2000) 593–610, [hep-ph/9905350].

[26] M. Benayoun, P. David, L. DelBuono and F. Jegerlehner, *An Update of the HLS Estimate of the Muon g-2*, Eur.Phys.J. **C73** (2013) 2453, [1210.7184].

[27] H. Leutwyler, *On the 1/N-expansion in chiral perturbation theory*, Nucl. Phys. Proc. Suppl. **64** (1998) 223–231, [hep-ph/9709408].

[28] R. Kaiser and H. Leutwyler, *Pseudoscalar decay constants at large $N_c$*, in Adelaide 1998, Nonperturbative methods in quantum field theory (2001) 15–29, [hep-ph/9806336].

[29] M. Bando, T. Kugo and K. Yamawaki, *On the Vector Mesons as Dynamical Gauge Bosons of Hidden Local Symmetries*, Nucl. Phys. **B259** (1985) 493–502.

[30] M. Benayoun and H. B. O'Connell, *SU(3) breaking and hidden local symmetry*, Phys. Rev. **D58** (1998) 074006, [hep-ph/9804391].

[31] M. Hashimoto, *Hidden local symmetry for anomalous processes with isospin/SU(3) breaking effects*, Phys. Rev. **D54** (1996) 5611–5619, [hep-ph/9605422].

[32] BELLE collaboration, M. Fujikawa et al., *High-Statistics Study of the $\tau^- \rightarrow \pi^- \pi^0 \nu_\tau$ Decay*, Phys. Rev. **D78** (2008) 072006, [0805.3773].

[33] L. M. Barkov et al., *Electromagnetic Pion Form-Factor in the Timelike Region*, Nucl. Phys. **B256** (1985) 365–384.

[34] CMD-2 collaboration, R. R. Akhmetshin et al., *High-statistics measurement of the pion form factor in the rho-meson energy range with the CMD-2 detector*, Phys. Lett. **B648** (2007) 28–38, [hep-ex/0610021].

[35] CMD-2 collaboration, R. R. Akhmetshin et al., *Measurement of the $e^+e^- \rightarrow \pi^+\pi^-$ cross section with the CMD-2 detector in the 370-MeV - 520-MeV cm energy range*, JETP Lett. **84** (2006) 413–417, [hep-ex/0610016].

[36] SND collaboration, M. N. Achasov et al., *Update of the $e^+e^- \rightarrow \pi^+\pi^-$ cross section measured by SND detector in the energy region 400-MeV $< \sqrt{s} <$ 1000-MeV*, J. Exp. Theor. Phys. **103** (2006) 380–384, [hep-ex/0605013].

[37] KLOE collaboration, F. Ambrosino et al., *Measurement of* $\sigma(e^+e^- \to \pi^+\pi^-\gamma(\gamma))$ *and the dipion contribution to the muon anomaly with the KLOE detector*, Phys. Lett. **B670** (2009) 285–291, [0809.3950].

[38] KLOE collaboration, F. Ambrosino et al., *Measurement of* $\sigma(e^+e^- \to \pi^+\pi^-)$ *from threshold to 0.85* $GeV^2$ *using Initial State Radiation with the KLOE detector*, Phys.Lett. **B700** (2011) 102–110, [1006.5313].

[39] KLOE COLLABORATION collaboration, D. Babusci et al., *Precision measurement of* $\sigma(e^+e^- \to \pi^+\pi^-\gamma)/\sigma(e^+e^- \to \mu^+\mu^-\gamma)$ *and determination of the* $\pi^+\pi^-$ *contribution to the muon anomaly with the KLOE detector*, Phys.Lett. **B720** (2013) 336–343, [1212.4524].

[40] BABAR collaboration, Bernard Aubert et al., *Precise measurement of the* $e^+e^- \to \pi^+\pi^-(\gamma)$ *cross section with the Initial State Radiation method at BABAR*, Phys. Rev. Lett. **103** (2009) 231801, [0908.3589].

[41] BABAR COLLABORATION collaboration, J.P. Lees et al., *Precise Measurement of the* $e^+e^- \to \pi^+\pi^-(\gamma)$ *Cross Section with the Initial-State Radiation Method at BABAR*, Phys.Rev. **D86** (2012) 032013, [1205.2228].

[42] Gerard 't Hooft, *How Instantons Solve the U(1) Problem*, Phys. Rept. **142** (1986) 357–387.

[43] PARTICLE DATA GROUP collaboration, J. Beringer et al., *Review of Particle Physics (RPP)*, Phys.Rev. **D86** (2012) 010001.

[44] G. Grayer et al., *High Statistics Study of the Reaction* $\pi^- p \to \pi^-\pi^+ n$: *Apparatus, Method of Analysis, and General Features of Results at 17-GeV/c*, Nucl. Phys. **B75** (1974) 189.

[45] S. D. Protopopescu et al., $\pi\pi$ *Partial Wave Analysis from Reactions* $\pi^+ p \to \pi^+\pi^-\Delta^{++}$ *and* $\pi^+ p \to K^+ K^- \Delta^{++}$ *at 7.1-GeV/c*, Phys. Rev. **D7** (1973) 1279.

[46] G. Colangelo, J. Gasser and H. Leutwyler, $\pi\pi$ *scattering*, Nucl.Phys. **B603** (2001) 125–179, [[hep-ph/0103088]].